

# Jamming creep of a frictional interface

L. Bureau, T. Baumberger, C. Caroli

*Groupe de Physique des Solides, Universités Paris 6 et 7, UMR CNRS 7588, 2 place Jussieu,  
75251 Paris, Cedex 05, France*

(October 31, 2018)

## Abstract

We measure the displacement response of a frictional multicontact interface between identical polymer glasses to a biased shear force oscillation. We evidence the existence, for maximum forces close below the nominal static threshold, of a jamming creep regime governed by an ageing-rejuvenation competition acting within the micrometer-sized contacting asperities. Quantitative analysis of the creep curves suggests that another such mechanism might be at work within the nanometer-thick adhesive junctions.

83.60.La, 62.20.Qp, 46.55.+d

Solid friction between two macroscopic solids is commonly characterized in terms of *(i)* a static force threshold below which no relative displacement is supposed to take place, *(ii)* a dynamic friction coefficient, measured in stationary motion. However, recent experiments performed on multicontact interfaces (MCI), *i.e.* interfaces between two solids with rough surfaces, pressed together under a load  $N$ , have revealed that [1]:

*(i)* for shear forces  $F$  such that  $F/N \ll \mu_s$ , where  $\mu_s$  is the static threshold, the pinned interface responds elastically, *via* the reversible deformation of the contacting asperities,

*(ii)* for  $F \lesssim \mu_s N$ , creeplike irreversible sliding is observed.

Clearly, the study of the latter regime of incipient sliding should give access to precise information about the underlying pinning/depinning dynamics.

It is now well established [2] that, for a MCI, the variations of the friction force  $F = \sigma_s \Sigma_r$  (with  $\Sigma_r$  the real area of contact, and  $\sigma_s$  the interfacial shear stress) are governed, at low velocities, by the competition between two effects: *(i)* an age strengthening effect resulting from the logarithmic creep growth, under the high (geometry-enhanced) normal load, of the sparse contacts between load bearing asperities. When motion starts, contacts get gradually destroyed, after a lifetime or age  $\Phi$ , and replaced by fresh ones. So, while the interface sits still, it ages (strengthens), when it slides, it rejuvenates (weakens). Full refreshment occurs, on average, after sliding a micrometric memory length  $D_0$ . *(ii)* Weakening when sliding is counteracted by the velocity-strengthening interface rheology:  $\sigma_s(\dot{x}) = \sigma_{s0} [1 + \alpha \ln(\dot{x}/V_0)]$ , with  $\dot{x}$  the instantaneous sliding speed. It results from thermally activated premature depinning events within the nanometer-thick adhesive junctions between contacting asperities.

Both effects yield logarithmic variations of  $F$ . One thus expects creep to exhibit a strong, exponential, sensitivity to forces close to the nominal static

threshold.

Now, the experiments reported in [1] were performed under static loading through a spring of finite stiffness. As such, they did not provide a force control fine enough to study incipient creep accurately. So, we have chosen, in this work, to probe it *via* the response to a biased *a.c.* shear force. With a bias  $F_{dc} \ll \mu_s N$ , and an amplitude such that the maximum force  $F_{max}$  lies in the tangential creep range, the interface should experience, during each oscillation period, an alternation of two regimes: (i) for  $F$  close to  $F_{max}$ , a sliding phase during which rejuvenation is at work, yielding an age variation  $\Delta\Phi_{slide}$ , and (ii) as  $F$  decreases, the slip velocity decreases quasi-exponentially, and the slider enters, for the rest of the period, a quasi static phase where age grows linearly with time by an amount  $\Delta\Phi_{stat}$ . Such a competition between rejuvenation and ageing is akin to that invoked to model soft glassy rheology (SGR) [3].

If, say,  $\Delta\Phi_{slide} + \Delta\Phi_{stat} < 0$ , the interface will weaken, leading to a larger slip during the next period, etc. One thus expects the dynamics to bifurcate between self-accelerated unlimited slip and self-decelerated, jamming [4], creep. The experiments reported below fully confirm this qualitative scenario. Moreover, quantitative analysis of the data, based upon the Rice-Ruina (RR) model [5], allows us to show that the rejuvenation-ageing process cannot be fully ascribed to variations of  $\Sigma_r$ , leading us to conclude that the interfacial rheology is most likely, itself, of the SGR type.

*Experiments.* — The experimental setup has been fully described in [6]; it is sketched in the inset of Fig.1a. Two poly(methyl methacrylate) (PMMA) samples, with lapped surfaces of roughness  $R_a = 1 \mu\text{m}$ , are glued on a slider and a track and form the multicontact interface. The slider, of nominal area  $4 \text{ cm}^2$ , rests on the track, inclined at  $\theta = 20^\circ$  from the horizontal. The tangential ( $F_{dc}$ ) to normal ( $N$ ) load ratio  $\gamma_{dc} = \tan \theta = 0.36$  is well below the

static threshold  $\mu_s \approx 0.6$  (see [2]) and no sliding occurs. Imposing a harmonic motion to the track then results in an inertial shear loading of the slider, of amplitude  $F_{ac} = \gamma_{ac}N$ , with  $\gamma_{ac} \leq 0.5$ . The frequency  $f = 80$  Hz is chosen well below the natural frequency of the slider-interface system,  $f_0 = 800$  Hz, so that the inertia associated to its relative motion in the track frame can be neglected. We measure the displacement  $X$  of the center of mass of the slider by means of a capacitive displacement gauge, with a noise amplitude 1 nm over its whole 0–500 Hz bandwidth. In order to prepare the system in as reproducible as possible an initial state, the slider is placed on the track and a large  $\gamma_{ac}$  is then imposed, in order to make it slide a few micrometers in the direction of  $F_{dc}$ . The harmonic force is then suddenly stopped, which results in an elastic recoil of the contacting asperities [7]. This method reduces the relative dispersion on interfacial stiffness values (see [6]) to only 10%. This value agrees with the expected statistical dispersion due to the finite number of load bearing contacts, which we can estimate to be of order 50. A time  $t_{wait}$  is then waited before reswitching the harmonic shear loading, either as a linear ramp of amplitude, until gross sliding occurs, or as a step with rising time  $\leq 0.1$  s.

*Results.*—The displacement response  $X(t)$  of the slider to a ramp  $\gamma_{ac}(t)$  is illustrated on Fig.1a. Also shown is the average displacement  $X_{dc}$  measured by filtering  $X(t)$  through a low-pass filter of cutoff frequency 8 Hz. In region (I), the slider oscillates about a constant average position, no irreversible slip occurs: the MCI responds elastically. Region (III) corresponds to accelerated sliding. In region (II) between these two regimes, the average displacement  $X_{dc}$ , *i.e.* the slipped distance, increases continuously. We use this ramp test to define a threshold  $\gamma_s = (F_{dc} + F_{ac})/N$  such that the average sliding velocity  $dX_{dc}/dt = 100 \mu\text{m.s}^{-1}$ . We thus obtain, for  $t_{wait} = 600$  s and  $\dot{\gamma}_{ac} = 0.1 \text{ s}^{-1}$ ,  $\gamma_s = 0.59 \pm 0.03$ . The scattering, of order 10%, is consistent with that of the

stiffness.

One can see, on Fig.1a, that the intermediate creep regime (II) corresponds to a narrow range of  $\gamma_{max} = \gamma_{dc} + \gamma_{ac}$ . Slow creep is studied by choosing a value  $\gamma_{max}$  in this range, setting, at  $t = t_{wait}$ , the amplitude stepwise to  $\gamma_{ac}$ , and recording  $X_{dc}(t)$ .

The set of creep curves displayed on Fig.1b all correspond to  $t_{wait} = 300$  s,  $\gamma_{max} = 0.54$ . The large dispersion between  $X_{dc}$  for various runs must therefore result from the statistical dispersion of the MCI initial state. After slipping by a finite amount, of order 10–100 nm, over the rising time (0.1 s) of  $\gamma_{ac}$ , the slider performs a slowly self decelerating creep. After, typically,  $10^4$  s, the slip velocity has decreased to non-measurable values, indicating a saturating, jamming dynamics. We attribute the large dispersion of the creep curves to the expected above-mentioned exponential sensitivity of the dynamics to  $\gamma_s - \gamma_{max}$ . A direct confirmation of this is obtained from the experiment presented on Fig.1c: it shows that a 3% step of  $\gamma_{max}$  turns quasi-jamming into accelerated sliding.

These ideas can be checked in a more quantitative way as follows: as long as the age of the MCI has not been appreciably modified by the creeping dynamics itself, we expect the characteristic time for creep,  $t_c$ , to be that for thermally activated depinning of a typical  $\text{nm}^3$  pinned unit within the adhesive layer:  $\ln(t_c) \sim Cst + \Delta E/kT$ , where  $\Delta E$  is the energy barrier to be jumped by an element under reduced load  $\gamma_{max}$ . Close to the depinning threshold [8]  $\Delta E/kT \sim (\gamma_s - \gamma_{max})/A$ . The RR rate parameter  $A = \alpha\sigma_{s0}/\bar{p}$ , with  $\bar{p}$  the average pressure on the microcontacts, has been measured, for PMMA/PMMA, to be 0.013 [9]. Hence, we expect the slipped distance in run (i) to scale as  $X_{dc}^i(t) = \tilde{X}(t/C_i)$ , where  $\ln(C_i) \sim (\gamma_s^i - \gamma_{max})/A$ . Fig.2 shows the set of creep curves resulting from such a scaling. Indeed, the collapse onto a master curve is very good in the short time range. Moreover, we find the

maximum spread of the scaling factors  $\max |\ln(C_i/C_j)| \approx 4.4$ , in excellent agreement with  $\max |\Delta(\gamma_s^i - \gamma_{max})|/A \approx 4.6$ .

*Discussion.*— We now analyze our results within the framework of the Rice-Ruina phenomenology [5], which has proved to account very well for the stick-slip frictional dynamics of MCIs [2]. It models the above described rejuvenation-ageing process and the velocity strengthening interface rheology as follows.

The friction coefficient reads:

$$\mu = F/N = \mu_0 + A \ln \left( \frac{\dot{x}}{V_0} \right) + B \ln \left( \frac{\Phi V_0}{D_0} \right) \quad (1)$$

$\Phi$  is the interface age,  $\mu_0$  the friction coefficient at reference velocity  $V_0$ . The instantaneous interfacial sliding velocity  $\dot{x}$  is related to the center of mass position by  $\dot{x} = d(X - F/\kappa)/dt$ , with  $\kappa$  the interfacial elastic stiffness [9].

The age  $\Phi$  evolves according to:

$$\dot{\Phi} = 1 - \frac{\dot{x}\Phi}{D_0} \quad (2)$$

On the r.h.s. of Eq.(2), the first and second terms correspond, respectively, to time ageing and slip rejuvenation.

We have performed numerical integrations of this set of differential equations to calculate the slipped distance  $X_{dc}(t)$  with, in Eq.(1),  $F/N = \gamma_{dc} + \gamma_{ac} \cos(\omega t)$ , and initial conditions for slip and age  $X_{dc}(0) = 0$ ,  $\Phi(0) = t_{wait} = 300$  s. We have used for the memory length  $D_0$  and the dimensionless parameters  $A$  and  $B$  the values  $D_0 = 0.42 \mu\text{m}$ ,  $A = 0.013$ ,  $B = 0.026$ , obtained from previous measurements on PMMA [9]. We choose  $V_0 = 1 \mu\text{m.s}^{-1}$ . Due to the exponential amplification by the creep dynamics of the small variations of the absolute friction level between various runs,  $\mu_0$  must be left free. This unique fitting parameter is tuned so as to adjust the calculated and measured values of  $X_{dc}$  at the end of the run. A typical example of such fits is shown on Fig.3. It yields  $\mu_0 = 0.42865$  [10], fully compatible with previous data [2].

These fits appear to be very good at long times  $t \gtrsim 1000$  s, that is in the quasi-jammed regime where static ageing becomes dominant. The corresponding asymptotic dynamics can be analyzed directly. From Eq.(1):

$$\frac{\dot{x}}{V_0} = \left( \frac{D_0}{V_0 \Phi} \right)^\beta \exp \left[ \frac{\gamma_{max} - \mu_0}{A} \right] \exp \left[ \frac{\gamma_{ac}(\cos(\omega t) - 1)}{A} \right] \quad (3)$$

with  $\beta = B/A$ .

Let us consider the oscillation period centered at  $t_1$ , with  $\gamma(t_1) = \gamma_{max}$ . The velocity  $\dot{x}$  only takes on significant values for  $\gamma \approx \gamma_{max}$ , *i.e.* for  $|\tau| = |t - t_1| \ll T$ . So, in Eq.(3),  $\cos(\omega t) - 1 \approx -\omega^2 \tau^2 / 2$ , and:

$$\frac{\dot{x}}{V_0} \approx \left( \frac{\Phi_c}{\Phi} \right)^\beta \exp \left[ -\frac{\tau^2}{\tau_c^2} \right] \quad (4)$$

with the constant  $\Phi_c^\beta = (D_0/V_0)^\beta \exp[(\gamma_{max} - \mu_0)/A]$  and  $\omega \tau_c = (2A/\gamma_{ac})^{1/2}$ .

To lowest order, the slip-induced  $\Phi$  variation can be neglected, and Eq.(2) yields:

$$\Phi \approx t + \Theta \quad (5)$$

where the integration constant  $\Theta$  is the age at some “initial” time within the quasi-jammed regime.

From Eqs.(4) and (5), the increment of slip over this period:

$$\Delta x \approx \int_{-\infty}^{+\infty} \frac{\Phi_c^\beta V_0}{(t_1 + \tau + \Theta)^\beta} \exp \left[ -\frac{\tau^2}{\tau_c^2} \right] d\tau \quad (6)$$

where the integration can be extended to infinity due to the gaussian decay of  $\dot{x}$ . Then, for  $t_1 \gg \Theta$ :

$$\Delta x \approx \frac{V_0 \Phi_c^\beta \sqrt{\pi} \tau_c}{t_1^\beta} + O \left( \frac{1}{t_1^{\beta+1}} \right) \quad (7)$$

From this, the sliding velocity  $\dot{X}_{dc}$ , coarse-grained over the period  $T$ :

$$\dot{X}_{dc}(t) \approx \frac{\Delta x}{T} \approx V_0 \sqrt{\frac{A}{2\pi\gamma_{ac}}} \frac{\Phi_c^\beta}{t^\beta} \quad (8)$$

and we obtain for the slipped distance:

$$X_{dc}(t) \approx Cst - \frac{V_0}{\beta - 1} \sqrt{\frac{A}{2\pi\gamma_{ac}}} \frac{\Phi_c^\beta}{t^{\beta-1}} \quad (9)$$

Since, for our system,  $\beta = 2$ , we thus expect the crept distance to approach its saturation level as  $1/t$ .

Our experimental data are seen on the insert of Fig.3 to fit the jamming asymptotics predicted by the RR model with excellent accuracy.

However, for all the experimental runs, we find (see Fig.3) that, although the overall shape of  $X_{dc}(t)$  is reasonably well described by the RR fits, the agreement is clearly not quantitative at short times ( $t \lesssim 1000$  s). In this time bracket, the RR model systematically underestimates  $X_{dc}(t)$ , hence the rejuvenation efficiency of slip. In particular, it by no means accounts for the fast increase of  $X_{dc}$ , which amounts typically to  $\sim 10\%$  of the total slip, occurring over the stepping time.

This strongly hints at the fact that the RR model, while it very well describes established sliding, misses some important feature of incipient sliding. We suspect that this missing feature might be slip-induced rejuvenation, *i.e.* dynamical weakening of  $\sigma_s$ , within the nanometer-thick adhesive junctions themselves. Indeed, these certainly have an amorphous solid structure when pinned, and they flow beyond a stress threshold. As such, they can reasonably be expected to behave as soft glassy materials, whose rheology is now interpreted [3] in terms of structural ageing/rejuvenation competition. If this turns out to be the case, two such mechanisms would be at work in the MCI solid friction, on the two scales of, respectively, the micrometric asperities, and the nanometric pinning units.

This issue is, in particular, of primary relevance to the modelling of the dynamics of interfacial shear fracture [11,12]. We plan to investigate it by studying the frictional dynamics of rough PMMA sliding over smooth hard glass. Since, with such a system, the microcontact population is unaffected



by motion, rejuvenation, if observed, will have to originate from the adhesive junctions.

## REFERENCES

- [1] P. Berthoud and T. Baumberger, Proc. R. Soc. London, Ser. A **454** 1615 (1998).
- [2] P. Berthoud, T. Baumberger, C. G'Sell, and J.-M. Hiver, Phys. Rev. B **59**, 14313 (1999).  
T. Baumberger, P. Berthoud, and C. Caroli, Phys. Rev. B **60**, 3928 (1999), and references therein.
- [3] S.M. Fielding, P. Sollich, and M.E. Cates, J. Rheol. **44**, 323 (2000), and references therein.
- [4] A.J. Liu and S.R. Nagel, Nature (London) **396**, 21 (1998)
- [5] J. R. Rice, and A. L. Ruina, J. Appl. Mech. **50** 343 (1983).
- [6] T. Baumberger, L. Bureau, M. Busson, E. Falcon, and B. Perrin, Rev. Sci. Instrum. **69**, 2416 (1998).
- [7] C. Caroli and Ph. Nozières, Eur. Phys. J. B **4**, 233 (1998).
- [8] Persson B. N. J., Sliding Friction: Physical Principles and Applications, Nanosciences and Technology Ser., Springer Verlag, Berlin, 1998, Chap. 11.
- [9] L. Bureau, T. Baumberger, C. Caroli, Phys. Rev. E **62**, 6810 (2000).
- [10] The five decimal places are necessary to adjust the final  $X_{dc}$  to 1%.
- [11] A. Cochard and J.R. Rice, J. Geophys. Res. **105**, 25891 (2000).
- [12] C. Caroli, Phys. Rev. E **62**, 1729 (2000).

## FIGURES

FIG. 1. (a) Instantaneous (line) and averaged ( $\bullet$ ) displacement response of the slider to a biased oscillating shear force of ramped reduced amplitude  $\gamma_{ac}(t)$  ( $\circ$ ). The bias  $\gamma_{dc} = 0.36$ . The arrow indicates the point at which the averaged velocity reaches  $100 \mu\text{m.s}^{-1}$ . Inset: experimental setup. (b) Recordings of the average creep displacement  $X_{dc}$  for four runs performed under identical nominal conditions:  $\gamma_{dc} = 0.36$ ,  $\gamma_{ac} = 0.18$ ,  $t_{wait} = 300$  s. The wide scattering of the curves results from dynamical amplification of the statistical dispersion of the interfacial strength. (c) Transition from jamming to unbounded slip ( $\bullet$ ) triggered by a 3% jump of  $\gamma_{max} = \gamma_{dc} + \gamma_{ac}$  ( $\circ$ ).

FIG. 2. Scaled plot of 7 creep curves (same nominal conditions as for Fig.1b). The reference run ( $C = 1$ ) corresponds to ( $\circ$ ) symbols.

FIG. 3. An experimental creep curve ( $\bullet$ ) and its fit according to RR model (line). With  $\gamma_{dc} = 0.36$ ,  $\gamma_{ac} = 0.18$ ,  $t_{wait} = 300$  s. Inset: the same plotted *versus*  $1/t$ , the dashed line indicates the quasi-jamming asymptotics (see text).

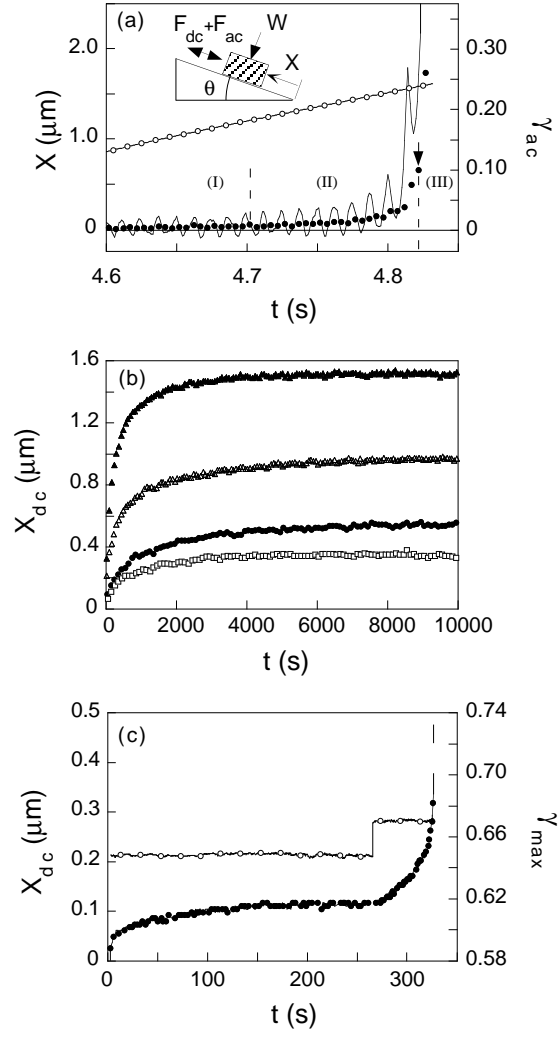


Figure 1:

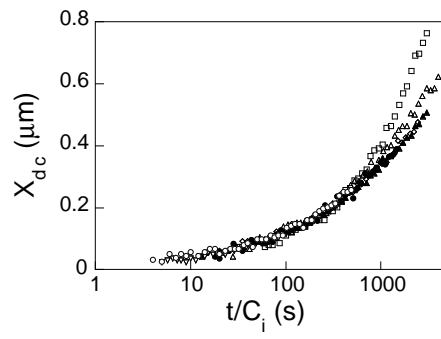


Figure 2:

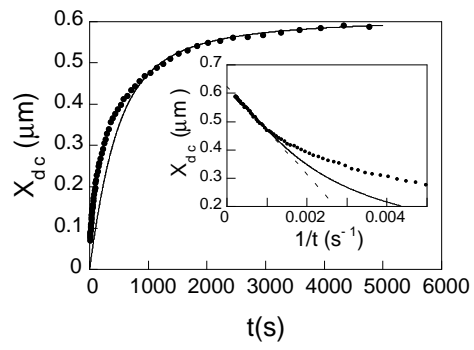


Figure 3: